Journal of Materials Chemistry C

ROYAL SOCIETY OF CHEMISTRY

REVIEW

View Article Online
View Journal | View Issue

Cite this: J. Mater. Chem. C, 2021, 9, 16132

Metal–organic framework based systems for CO_2 sensing

Andreea Gheorghe, Olivier Lugier, Bohui Ye and Stefania Tanase *

Received 15th May 2021,
Accepted 3rd August 2021

DOI: 10.1039/d1tc02249k

rsc.li/materials-c

Monitoring CO_2 levels in the atmosphere as well as in work place environments is strictly regulated. Commercial sensors based on polymeric materials have low operating temperature, yet exhibit low selectivity. Molecular systems such as metal–organic frameworks (MOFs) are promising materials that can be used for CO_2 sensing applications. They are formed through strong interactions between metal ions or clusters with easy-to-modify organic linkers and have exceptionally high surface areas and well-defined accessible pores. The host–guest interactions in MOFs and their responsiveness to physical and chemical stimuli can be exploited to address the critical issues in chemical sensing applications, such as fast response, sensitivity and specificity. This review provides an overview of the techniques that can be used to detect CO_2 through the use of MOFs, highlighting the most promising MOF materials that exhibit CO_2 sensing properties. The potential of MOFs in the development of CO_2 sensors is also discussed.

Introduction

Global warming is primarily caused by emissions of CO_2 and other harmful gases (NO_x, SO_x, and volatile organic compounds) into the atmosphere, and it mostly comes from human activities through industries and vehicles.[1] The research station of the National Oceanic and Atmospheric Administration (NOAA) of the U.S. Department of Commerce started measuring CO_2 levels in the late 1950s when the atmospheric CO_2 concentration was at around 315 ppm.[2] On the 8th of April 2021, the daily average of CO_2 levels was 421 ppm, the first time in human history that the number has been so high.[3] Whereas rising carbon dioxide levels in the atmosphere cause great concern worldwide, most of us pay little to no attention to risks posed by CO_2 changes indoors. Recent studies show that decision-making and other cognitive abilities decline at elevated indoor CO_2 levels due to inadequate ventilation in buildings.[4] Despite the fact that we breath in and out carbon

Van't Hoff Institute of Molecular Sciences, University of Amsterdam, Science Park 904, 1098 XH, The Netherlands. E-mail: s.grecea@uva.nl

Andreea Gheorghe

Andreea Gheorghe obtained a BSc (2013) and MSc (2015) in Chemistry, both from the University of Bucharest. She obtained her PhD in Chemistry (2020) from the University of Amsterdam. Her work focused on the rational design of homochiral metal–organic frameworks for enantioselective catalysis. Currently, she is a postdoctoral researcher at the University of Amsterdam where she develops methods for the integration of MOFs on electrode surfaces for applications in electrocatalytic conversion and sensing of CO_2.

Olivier Lugier

Olivier Lugier obtained his BSc (2014) in Chemistry and MSc (2016) in Materials Chemistry at the University of Angers. From 2016 to 2021, Olivier worked on his PhD project at the University of Amsterdam and at the Advanced Research Center for Nanolithography (ARCNL) in Amsterdam. His research focused on exploring new nanopatterning processes for extreme ultraviolet lithography using metal–organic frameworks and self-assembled monolayers as photoresists. Currently, he is a postdoctoral researcher at the University of Amsterdam and VU Amsterdam where he focuses on the development of molecular-based sensors for chemical sensing.

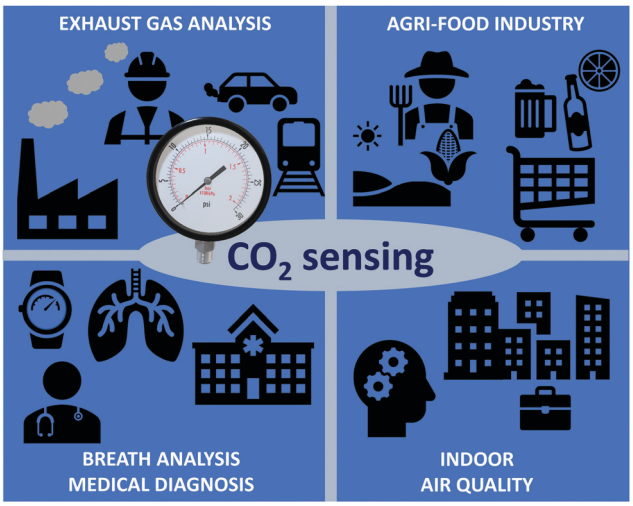

Fig. 1 CO_2 sensing in different fields.

dioxide, the maximum safe level of carbon dioxide is at 5000 ppm. Above the safe CO_2 level, it can cause symptoms such as fatigue, headache, anxiety, loss of energy, jelly legs and lung ventilation problems.[5] Therefore, it is of utmost importance to have reliable CO_2 sensors which can be used in health and safety applications, including surveillance and air quality (low CO_2 levels) as well as by industries that produce CO_2 (high CO_2 levels) in order to protect their workers from the harmful effects of augmented CO_2 levels (Fig. 1).[6]

Commercial CO_2 sensors are classified in two major types: nondispersive infrared (NDIR) optical and chemical sensors. A NDIR sensor uses an infrared beam that does not scatter upon interaction with guest molecules. The NDIR CO_2 sensor measures the abundance or concentration of CO_2 through the partially absorbed light by CO_2 when CO_2 is between the IR light source and detector. Since the concentration of gases is proportional to the transmission of the IR beam, the change of the IR beam intensity is small when the concentration of CO_2 is low and therefore, it can fall below the detection capacity of the detector. This results in high detection limit in NDIR sensors. A typical NDIR CO_2 sensor has a detection limit of 0.2 ppm with an accuracy of $\pm$30 ppm.[7] NDIR sensors usually operate between 1 and 10 μm,[8] a range in which the absorption of water vapour occurs. Since CO_2 gas detection is often carried out in conditions where water vapour is present, water vapour interference is one of the biggest challenge when NDIR sensors are used to detect CO_2.[9] Absorption interference caused by water vapor or other molecules can be (partially) solved using optical filters and interference correction. However, by using optical filters, the spectral absorption of CO_2 is drastically reduced due to refractive property of the optical filter. Additionally, using optical filter increases the price of the NDIR sensors.[10]

Commercial chemical CO_2 sensors consist of a sensing layer made up by polymers that operate at room temperature. Polymers used for CO_2 detection often contain amine groups. The sensing principle of these amine-based polymers is based on an acid–base reaction.[11,12] The interaction between CO_2 and amine groups is reversible and it involves the formation of ionic species. This interaction is an acid base equilibrium, and the sensing mechanism of polymer-based CO_2 sensors is based on the pH change upon the reaction of amines with CO_2 to form carbamates and cationic species of ammonia or amine. During this process, carbamic acids are formed as intermediates. Carbamates formed during the acid–base reaction are thermal unstable molecules and CO_2 can be released upon heating, allowing to re-use the active sites of the polymer-based sensors.[11]

Advantages of polymer-based sensors include high sensitivity, short response time, low power consumption and small size, allowing for portable use.[13] Nevertheless, the main

Bohui Ye

Bohui Ye obtained his BSc (2016) and MSc (2019) degree in chemistry at the University of Amsterdam. During 2018–2019, he worked on his MSc thesis under the supervision of Dr S. Tanase at the University of Amsterdam. His research focused on the synthesis of metal–organic frameworks and their application for CO_2 sensing at ambient condition.

Stefania Tanase

Stefania Tanase (Grecea) is associate professor in Functional Materials at the University of Amsterdam. She received her BSc (1996) from the University of Bucharest and her MSc (1997) from the Polytechnic University of Bucharest. She obtained her PhD (2002) from the University of Bucharest, for which she received a Young Investigator Award. She joined the University of Amsterdam after a postdoc (2001–2004) and independent NWO-VENI research fellow (2005–2008) at the University of Leiden. Her current research focuses on the design of materials and devices for applications in molecular separations and chemical sensing, proton conductive membranes and catalysis.

drawbacks are the poor selectivity and short and long-term sensor drift that lead to inaccurate measurements over time. Therefore, polymer-based sensors are calibrated prior the shipment, overtime and the zero point needs to be recalibrated to maintain long-term stability.[14] Metal oxide sensing layers have emerged as a promising choice in the gas sensor industry.[15] Their working principle is based on the redox reactions between the target gas and the oxygen species bound on the surface of the metal oxide.[16] Reaction of these oxygen species with reducing gases or a competitive adsorption and replacement of the adsorbed oxygen by other molecules lead to an increased conductivity. The oxygen species are believed to be dominant at operating temperature of 300–450 °C which is the working temperature for most metal oxide gas sensors.[15] The limitations resulting from such high temperatures include poor selectivity (cross-sensitivity) and baseline drift.[17,18]

A comprehensive account of commercial sensing materials for CO_2 sensor devices, including their properties and relative advantages has been reported in literature.[19] Emerging sensing materials include carbon nanotubes (CNTs),[20] graphene,[21] MoS_2,[22] zeolites[23] and metal–organic frameworks (MOFs).[24] Among them, MOFs are the preferred choice because their structure can be tailored to enhance the selectivity towards a target analyte, and to tune the interplay between structure and properties.[25–27]

MOFs are porous materials composed of metal ion nodes and organic linkers (Fig. 2).[28] Their modular nature allows for great synthetic tunability, affording both fine chemical and structural control. They have unique characteristics, being able to take-up, hold and release molecules from their pores in a selective manner. Their high surface area to volume ratio is especially beneficial for sensing applications as the high surface area to volume ratio enhances the chance of interaction between the sensing materials and analytes, which leads to high sensitivity. The properties of MOFs beyond those of traditional sensing materials include adsorption properties tailored to specific analytes,[26] tunable dielectric properties,[25] intrinsic porosity that allows through-solid mass and ion transport, mechanical properties in between polymers and inorganics[29] and electronic conductance tailored from practically zero to over a hundred S cm^{-2}.[30]

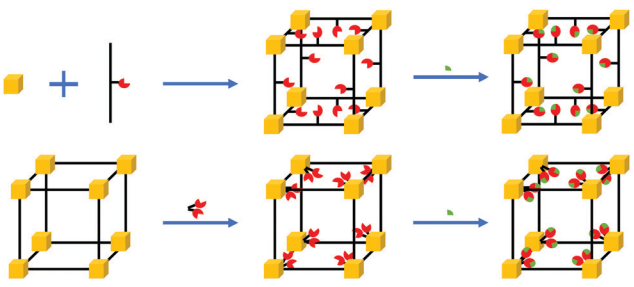

Fig. 2 A representation of synthetically modified MOFs to promote selective CO_2 adsorption. Metal nodes (ion or cluster) with open metal sites (yellow), organic linker (black), CO_2 molecules (green), CO_2 binding sites (red).

The potential of MOFs for CO_2 capture and storage has been studied in great detail.[31,32] The selective adsorption of CO_2 molecules in the pores of MOFs is achieved by using different synthetic strategies for the design of MOFs. They involve the choice of specific organic linkers, use of open metal sites and the incorporation of functional groups inside the framework (Fig. 2).[33] Therefore, the pores of MOFs can act as molecular sieves.[34] By varying the metal ions and organic linkers, the window and pore size can be tuned to achieve selective adsorption of CO_2, leaving out undesired interactions inside the framework.[35] Fine tuning of the selective adsorption of MOFs allows for developing MOFs as sensing layers for accurate detection of CO_2 levels as well as their integration in chemical sensors.[36,37] This review discusses the working principle of MOF-based sensors used for CO_2 detections, highlighting the *pros* and *cons* of MOF materials. Since the integration of MOFs as thin-films in sensor devices requires to prepare micro- or/and nano-scaled MOF crystals which have controlled size, shape, and morphology, we also present the common fabrication techniques for MOF thin-films on electrode surfaces and assess their practical applicability.

CO_2 sensing using MOFs

Sensor devices require two main constituents: a sensing layer and a transducer (Fig. 3). The sensing layer interacts selectively with the target analytes, so that various changes in the physicochemical properties of the system (*e.g.*, capacitance, mass, conductivity, optical properties, *etc.*) are detected. The transducer translates the changes in measurable signals.

The advantage of MOFs over traditional sensing materials comes from their capacity to concentrate the target analyte within their pores, acting like a sponge with astonishing surface to volume ratio, and their potential selectivity for specific analytes that can be adjusted by tuning the structure and/or chemical composition of the MOF. In such MOF-based sensing devices, the transducer component usually provides information related to variations in mass, electronic properties or

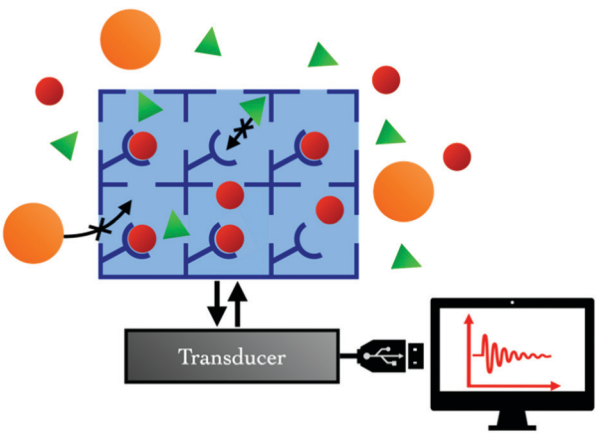

Fig. 3 The principle of MOF-based chemical sensing.

Table 1 CO_2 detection using MOFs as sensing layers

MOF	Transduction approach	Range tested LoD	Response/recovery time	CO_2 selective	Water stability	Potential for other analytes	Ref.
ZIF-8	Fabry–Perrot cavities	0–100 vol% LoD: 0.019 vol% (1 Hz low-pass filtering)	<0.15 s/<0.30 s (≈ 3 s for 1 mL min^{-1} flow rate)	Yes (size selective)	High	Yes	39
ZIF-8	SEIRA	0–100% vol% LoD*: 52 ppm	—/—	Yes (size selective)	High	Yes	43
ZIF-8	SERS	— to — LoD: 5×10^{-8} M	8 min/—	Yes (size selective)	High	Yes	44
HKUST-1	IR absorption (optical fibres)	20 ppm to 100 vol% LoD: 20 ppm	10 s/106 s (100 vol%) 12 s/530 s (30 ppm)	No (H_2O, N_2)	Low	Yes	49
Mg-MOF-74 (chemically tuned)	Permittivity	200 to 5000 ppm LoD: 200 ppm	Minutes/—	No	Low	Yes	26
Co-MOF-74 (chemically tuned)	Electrical conductivity	100% (30 mL min^{-1}) LoD: —	200 s/—	No (CH_4, N_2, H_2O)	Low	Yes	54
Cu3(hexaimino benzene)2	Electrical conductivity	400–2500 ppm LoD*: 67 ppm	7–8 min (0% RH) 10–11 min (80% RH)	—	High	Yes	55
Al-MIL-53 + conductive carbon	Electrical conductivity	75 vol% (in CH_4) 100 vol% LoD: —	30 s	Yes (over CH_4)	High	Yes	25
CDMOF-2	Electrochemical impedance spectroscopy	0–100 vol% LoD: <10 vol%	—/—	Yes	High	Yes	62
Zn-MOF-74	Impedance	0–2000 ppm LoD: 500 ppm	—	Low	Medium	Yes	57
NH_2-M-MOF-74	Kelvin probe	400–4000 ppm LoD: —	—	— (H_2O sensitive)	Medium	Yes	68
MAF-34	Luminescence	— —	—/—	—	High	Yes (benzene, nitrobenzene, ethanol)	70
UiO-66-ONa (tuned UiO-66)	Luminescence (colorimetry)	— to — LoD: 3.5×10^{-7} M	~ 67 s/—	Yes	High	Expected	71
ZIF-8	Bimodal waveguide interferometry	1–100 vol% LoD: 3130 ppm (RT) 774 ppm (278 K)	<10 s	Yes (over H_2O, CH_4)	High	Yes	72
$Cu_2(nbdc)_2(dabco)$	Mass (QCM)	10–100 vol% LoD: 10 vol% (56% RH)	Seconds/seconds	Yes (over O_2, N_2, H_2, CH_4)	Medium	Expected	73
HKUST-1	LSPR spectroscopy	0–100 vol% LoD: 10 vol% LoD*: $\ll 10$ vol%	Few seconds (10 vol%)	—	Low	Yes (tested for SF_6)	74

LoD* = estimated or extrapolated LoD; — = information not provided by the authors.

optical properties.[38] In the following sections, we will discuss the transducer types which have been studied so far for CO_2 detection using MOFs as sensing layers (Table 1).

Refractive index (RI) sensing

Although the variations of CO_2 concentrations only trigger negligible change in refractive index multiple techniques involving MOFs have been developed to take advantage of this phenomenon. Kim *et al.*[39] reported a CO_2 sensor with a dynamic range of 0 to 100 vol% of CO_2 and a resolution of 0.019 vol%. Their sensor consists of two fibre-optic terminated with Fabry–Perrot (FP) cavities[40] made of thin films of ZIF-8, or $[Zn(melm)_2]$ where melm = 2-methylimidazolate, of different thickness for each fibre-optic. The reflection spectrum of each FP cavity depends on their dimension (*i.e.*, the thickness of the MOF thin film) and respective refractive index, which depends on the concentration of CO_2 molecules present in the films of ZIF-8. By combining two precisely tailored FP cavities, the authors were able to obtain a differential response to the changes in the refractive index of the system which enables low limit of detection (LoD) and a high resolution. This sensor shows multiple advantages such as its small size and straightforward fabrication method (dip-coating) that allows batch production. Furthermore, this method can potentially be adapted to detect any gas by replacing ZIF-8 with different types of MOF displaying affinities for other analytes.

Other studies focused on combining MOFs and surface plasmon resonance spectroscopy to monitor small changes in CO_2 concentrations. Surface plasmon resonance (SPR) is the coherent oscillation of conduction band electrons at the interface of a metal and a dielectric material upon light exposure. The resonance frequency of surface plasmons is closely related to the refractive index of the system. Hence, the phase and intensity values of the light reflected at the aforementioned interface can be used to obtain information on the RI, and thus, on the composition of the dielectric material.[41,42]

Chong *et al.*[43] proposed a complex sensor in which surface plasmon polaritons (SPP) are created by shining light onto a suspended silicon nitride (SiN_4) window on top of which, specially designed gold nanoarrays were patterned and covered by a film of ZIF-8. By tuning the properties of the SiN_4 window, the gold nanoarrays and the MOF layer, the authors were able

to match the resonance frequency of the SPPs to a specific CO_2 infrared absorption band resulting in a calculated enhancement factor of *ca.* 1800×. Despite the lower enhancement performances of their prototype compared to the model, due to imperfect testing conditions, the authors estimated its LoD at 52 ppm. The intricate design and working principle of this sensor could become a liability for a successful transitioning from numerical models or laboratory prototypes to mass-produced devices. Nevertheless, these results prove that surface-enhanced infrared absorption (SEIRA) can be used to fabricate highly sensitive CO_2 detectors. Furthermore, like the above-mentioned sensor based on double Fabry–Perrot ZIF-8 cavities, this device could detect other gases provided that the resonance frequency of the SPPs can be tuned to overlap with a characteristic infrared absorption band of the target analyte.

Huang *et al.*[44] proposed a similar method that combines the CO_2 absorption capacity of ZIF-8 films with localised surface plasmon (LSPP) resonance from gold nanoparticles on silver nanowire to develop a surface enhanced Raman scattering (SERS) based sensor. The authors could mould the silver nanowires together to form free-standing films of the CO_2 sensing material. Again, the LSPP acts as signal enhancer while extra thin films (1 nm to 3 nm) of ZIF-8 are used to selectively concentrate CO_2 molecules. A promising LoD of 5×10^{-8} M was obtained with a response time of eight minutes. Although only demonstrated as a proof of concept, such SERS-based sensor could virtually detect any analyte at low concentration, provided that it has distinctive Raman bands and displays affinity for the MOF used. Yet, the restrictions imposed by the thickness of the MOF layer (3 nm maximum) are expected to limit the number of compatible MOFs. Indeed, the current synthesis methods used to fabricate MOF thin films require improvements to gain precise control over the main properties of the material. Nevertheless, the versatility of Raman spectroscopy and the relative ease of fabrication (when using ZIF-8) of the proposed prototype are two enticing arguments in favour of such sensor.

Spectral near infrared sensing

Infrared (IR) sensors are commonly used to detect and identify gases. Most of the analytes absorb IR radiations at specific wavelengths in direct relation with their chemical composition (*i.e.*, their chemical bonds). The subsequent absorption bands can be used to detect and quantify the presence of the target analyte in a specific surrounding.[45,46] Although most commercially available mid-IR sensors are too large for portable use, optical fibres offer relatively cheap and convenient alternative for the fabrication of portable IR gas detectors.[47] The challenge of using optical fibre near infrared (NIR) sensors is that the gases do not have fundamental vibration bands at NIR regions. The detection must arise from the overtones of the fundamental vibration bands.[48] A fundamental vibration is excited by absorbing the (vibrational) quantum energy by a molecule in its ground state. When two of such quantum energies are absorbed, the first overtone is excited, and so on to higher overtones. Overtones from the fundamental vibrational bond

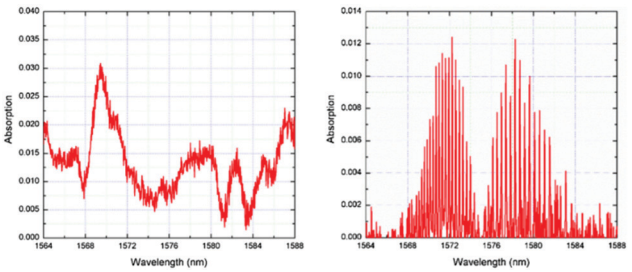

Fig. 4 Absorption spectrum of CO_2 confined within HKUST-1 (left) and of reference CO_2 gas inside quartz gas cell (right).[49]

that absorbs at the mid-IR frequency are generally weak. Thus, NIR sensors have low detection sensitivity.

Enhanced absorption can be achieved by increasing the optical path *via* optic fibres of several meters length or by using reflecting mirrors.[50] Alternatively, the cladding of the optical fibre can be removed by etching to allow coating with a sensitive layer to extend the light path and make use of evanescent wave absorption in order to achieve high reasonable detection.[48,51,52] For example, Chong *et al.*[49] have developed an ultra-short NIR fibre-optic CO_2 sensor by depositing a thin layer of HKUST-1, or $[Cu_3(btc)_2(H_2O)_3]$ where btc = benzentricarboxylate, on the core of an optical fibre. The MOF thin film was grown on the 5 cm-long etched single mode fibre through a layer-by-layer (LbL) method. When CO_2 selectively interacts with the HKUST-1 layer *via* unsaturated open Cu^{2+} metal sites, the refractive index of the sensing layer draws closer to the refractive index of the fibre and a larger portion of light propagates into the film, which is in direct correlation with CO_2 concentration. Fig. 4 shows the absorption spectrum obtained by Chong *et al.*[49] The reference CO_2 spectrum exhibited both vibrational bands and rotational fine lines. The missing rotational fine lines of the absorption spectrum of the CO_2 within HKUST-1 was attributed to tightly confined CO_2 molecules with no freedom of rotation.[49] Using their HKUST-1 coated single-mode optical fibre, the authors were able to develop a CO_2 sensor with a detection limit down to 20 ppm. The main drawbacks of such sensor at low CO_2 concentrations originate from its low adsorption and desorption kinetics. This was attributed to the adsorption mechanism of the gas within the MOF framework. At low concentrations, the gas chemisorbs onto the unsaturated metal sites, as opposed to a physisorption when detecting high CO_2 concentrations.[49]

Chemiresistive and chemicapacitive-based sensing

Physicochemical systems such as MOFs possess energy storage and dissipation properties. Electrochemical sensing examines these MOF properties translated as electric capacity and resistance.[53] Capacitance is described by the electrical charge storage at a certain potential. In chemical capacitive sensors, the dielectric constant or permittivity of the MOF as a function of time is monitored upon adsorption of CO_2.

Zhao *et al.*[26] reported the on-chip solvothermal growth of MOF films onto Pt interdigitated electrodes. The sensor was used for the detection of benzene and CO_2 at room temperature. LoD for CO_2 of both pristine and ethylene diamine modified Mg-MOF-74, also known as $[Mg_2(dobdc)(H_2O)_2]$ where dobdc = 2,5-dihydroxy-1,4-benzenedicarboxylate, was 200 ppm. An enhanced capacitive response by 25% was reported for the ethylenediamine functionalized Mg-MOF-74 material which corelates to a higher amount of gas adsorbed due to the basicity of the amine groups coordinated to the open metal sites. It was shown that the sensor is still stable after 3 weeks storage and has a reversible behaviour upon exposure to inert gas. Overall, this study demonstrates that custom-tailored amine–CO_2 interactions can be used as an effective strategy to enhance the sensitivity toward CO_2.

In the case of chemiresistive gas sensing, changes in the electronic resistance of the MOF sensing layer are monitored. Yet, the major bottleneck in the design of MOF-based chemiresistive gas sensors is the synthetic challenges associated with the organic linkers commonly used for electrically conductive or semiconductive MOFs. To overcome this, Caro *et al.*[54] prepared MOF-74 composites through gas-phase incorporation of organic semiconducting molecules, such as 7,7,8,8-tetracyanoquinodimethane (TCNQ) and tetrathiafulvalene (TTF). To assess the CO_2 sensing of these composites, the electrical current was measured as a function of the applied voltage under CO_2 atmosphere. An increased electrical conductivity was observed for the Co-MOF-74 containing TTF as compared to the bare Co-MOF-74 and the TCNQ loaded Co-MOF-74.[54] The response time was within *ca.* 200 s. This behaviour might be related to the interaction between TTF and Co-MOF-74, proposed to be based on through-bond conduction, but the electron conduction may also take place through the π–π stacking network.[54] The phenomenon reported and characterised in this study is of high relevance for CO_2 sensing.

Dinca *et al.*[55] have demonstrated the sensing of CO_2 at ambient conditions by using a 2D framework with a high density of NH moieties, namely Cu_3(hexaiminobenzene)$_2$, in a broad relative humidity (RH) range (*i.e.* 10% to 80% RH). The sensor was prepared by simple drop-casting of as-synthesized polycrystalline material onto interdigitated electrodes. Its stable response independent of the humidity was attributed to the acid–base adducts and bicarbonate salt formation at the organic–inorganic node of the MOF upon exposure to CO_2. The sensor device has a robust performance and good repeatability (*ca.* 7 days) at levels of CO_2 ranging from outdoor atmospheric level (400 ppm) up to limits typically found indoors (2500 ppm). Although the sensor sensitivity has drifted over time, as is generally observed for other chemiresistors, it still remained RH-independent after three months. Despite these promising results which reveal the potential of 2D MOFs in tuning and optimising chemiresistive responses, the synthesis of conductive 2D MOFs remains synthetically challenging and limited to conjugated benzene rings and porphyrin rings.[56]

To circumvent the low conductivity of MOFs, composite materials have also been synthesised.[25,57] Kaskel *et al.* prepared conductive carbon composites films comprising Al-MIL-53, also known as $[Al(OH)(bdc)]_x$ where bdc = 1,4-benzenedicarboxylate.[25] The sensor device includes a dried paste containing carbon black or single walled carbon nanotubes and polytetrafluoroethylene (PTFE) which are placed as a film on glass slides using silver conductive paint. The sensing principle used is based on the change of the conductivity near the percolation threshold of the composite material as a result of the well- known breathing effect of Al-MIL-53 framework. Upon CO_2 adsorption, MOF crystals expand at a specific pressure. Consequently, the percolating network created by the conductive additive, that allows electrons to flow through the composite, is disrupted. This causes the specific resistance of the material to increase which translates in a sudden decrease in the electrical conductivity (Fig. 5).[25] The response time of Al-MIL-53/conductive carbon sensors was below 30 s at partial pressure of CO_2 up to 6 bar. It was shown that using different carbon materials affects the response time, *i.e.* small isotropic particles of carbon black led to shorter response time as compared with highly anisotropic carbon nanotubes.[25]

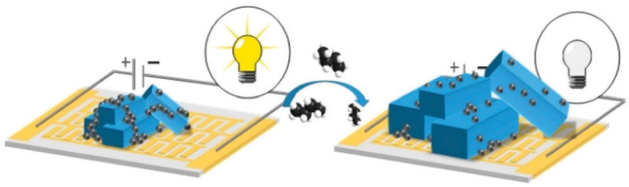

Fig. 5 Switchable MIL-53-carbon additive composite for CO_2 sensing.[25]

Impedance-based sensing

The existence of electrically conductive and semi-conductive MOFs has been the primary reason behind exploiting MOFs for sensing of gases and/or vapours.[58] Using impedance spectroscopy, the requirement of the sensing material to possess high electrical conductivity is circumvented because the electrical impedance of a MOF-based sensing layer can be measured over a range of frequencies of an applied electrical current. Furthermore, impedance-based sensors bring also advantages in terms of their low-cost, small size and highly interchangeable features.

It is well known that MOFs containing hydroxyl functional groups in their frameworks release protons into their nanopores or nanochannels with relatively low activation energies and thereby exhibit proton conduction.[59,60] This property can be exploited in CO_2 sensing since the adsorption of CO_2 can alter the concentration of protons which leads to changes in the proton conduction properties.[61]

Gassensmith *et al.*[57] reported a Rb-based MOF, containing γ-cyclodextrin as organic linker, to be an effective CO_2 sensing material due to the change of ionic conductivity upon its reaction with CO_2. This MOF, namely CDMOF-2 or $[(C_{48}H_{80}O_{40})(RbOH)_2\ (CH_2Cl_2)_{0.5}]_n$, covalently binds CO_2 to the non-coordinated free primary hydroxyl groups of its linkers, forming alkyl carbonic acid functional groups on the glucose unit (Fig. 6). Because carbonic acids are more acidic than primary alcohols, one would expect that the CO_2-bound CD-MOF-2 will

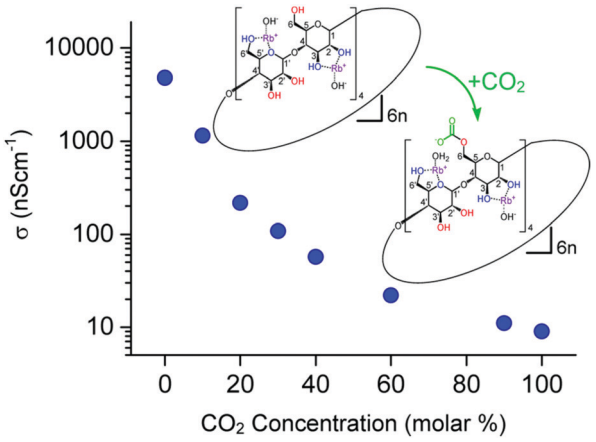

Fig. 6 Variations in the conductivity of CDMOF-2 upon CO_2 absorption/desorption cycles.[62]

show higher conductivity than pristine CD-MOF-2. Such behaviour would be expected due to easier release of the proton on alkyl groups as compared to alcohols. Surprisingly, the conductivity of CDMOF-2 decreased by a factor of ~550 after CO_2 sorption as a result of increased steric hindrances of the primary alcohol groups with the carbonates.[62] This sensor has a detection range from 0 vol% to 100 vol%. It was also shown that the chemical reaction is reversible over multiple cycles without affecting the sensor performances (Fig. 7).

Impedance CO_2 sensors were also fabricated using MOFs known for their selective CO_2 adsorption and high proton conductivity properties, namely Zn-MOF-74 and NdMo-MOF, or $[Nd(mpca)_2Nd(H_2O)_6Mo(CN)_8]\cdot nH_2O$ where mpca = 5-methyl-2-pyrazinecarboxylate.[61,63,64] The sensors were fabricates by mixing MOF powders with polyvinylpyrrolidone (PVP) and deposited as thin films on Pt sensors *via* drop casting. Both sensors gave a response upon changing the CO_2 concentration. Notably, the Zn-MOF-74 sensor showed low cross-sensitivity when changing the CO_2 concentration from 0 to 2000 ppm at different RH: 40%, 50% and 60%.[61] Same sensor also exhibits a fast response when the CO_2 concentration changes from 0 to 500 ppm at 50% RH. Although the exposure to synthetic air led to sensor deactivation cause by the presence of oxygen, the process is reversible upon exposure to inert conditions.[61]

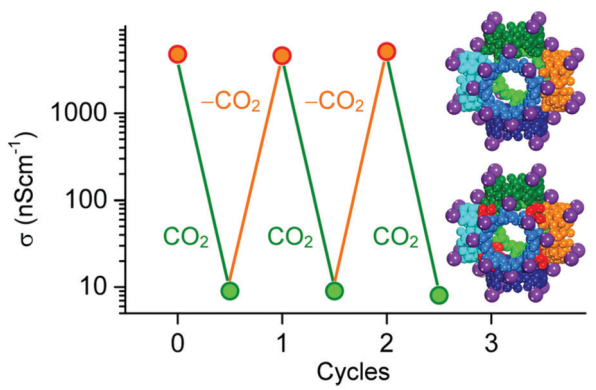

Fig. 7 Graph of the average conductivity values of CDMOF-2 as a function of the CO_2 concentration in N_2 atmosphere. The structural change of the MOF's γ-cyclodextrin (γ-CD) linker upon reaction with CO_2 is also shown.[62]

Field effect transistors and Kelvin probe

Sensors based on field effect transistors (FET) measure the electrical signal variations of the sensing material due to changes in its work function induced by the interaction with the target analyte.[65] The work function of a system represents the energy required to release electrons from a material's surface. Changes in a material's work function can be transduced using Kelvin probes.[66] These vibrating capacitor devices measure the contact potential difference between the sensing material and a reference material as electrons flow from the material with the lowest work function to the other.[67]

Pentyala *et al.*[68] studied the CO_2 sensing properties of various M-MOF-74 (M = Mg, Co, Zn or Ni) materials by using a Kelvin probe to detect the variations in the work function of the system upon interaction with CO_2. The materials tested share identical crystalline structures comprising pores of a relatively large diameters and, more importantly, free coordination sites on their metal centres. Once in the pores, the CO_2 molecules coordinate to the metal cations effectively and alter the electronic properties of the material, such as its work function. By monitoring these fluctuations, one can extrapolate information on the CO_2 concentration in the environment of the device. Successful CO_2 detection was obtained with each M-MOF-74 tested, although sensing was heavily influenced by humidity levels. The authors further investigated the potential of MOF-74, by functionalizing the pores of the Mg-based analogue with ethylene diamine *via* post-synthetic procedures. In this MOF analogue, referred to as NH_2-Mg-MOF-74, one of the amine groups of the ethylene diamine coordinates to the metal centre, while the other is oriented towards the inside of the pore. The free amine moiety can react with adsorbed CO_2 molecules through reversible acid–base reactions which also leads to changes in the work function (Fig. 8a). NH_2-Mg-MOF-74 displays significantly better sensing performances than Mg-MOF-74, particularly under humid conditions as the selectivity of the amine for CO_2 exceeds that of the metal centres. Interestingly, both the NH_2-Mg-MOF-74 and M-MOF-74 materials exhibit reversible behaviour.[68] This work successfully proves the potential of MOFs for CO_2 sensing by using work function measurements. The current LoD remains uncertain and, as mentioned by the authors, the unmodified MOFs have shown poor stability under humid conditions as was to be expected based on the hydrophilic nature of their metal centres and tendency to hydrolyse. Nevertheless, by taking advantage of the chemical tuneability of MOFs, the authors were able to redesign their sensing material to increase both the stability and performances of the sensors.

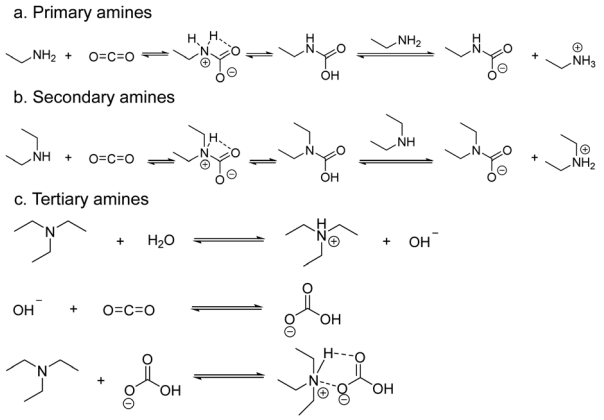

Fig. 8 The formation of carbamates upon interaction with CO_2 of primary (a), secondary (b), and tertiary amines (c).[11]

Luminescence-based sensing

Luminescence describes the emission of light that occurs in certain systems following the cold excitation of their electrons, triggered by the absorption of an incident photon of a specific energy, to higher electronic states (Fig. 9).

Due to their hybrid nature, MOFs often display two photon-emitting components, namely their organic linkers and metal ions. Moreover, additional emitting components can be added to the framework by loading its pores with luminescent guests. The interactions between the metal centres or linkers of the MOF and the guest molecules within its pores influence the luminescence properties. Such variation in the luminescence of the material can be measured and it provides detailed information on the concentration of specific guest molecules in the surrounding environment.[69]

Qi *et al.*[70] designed a sensor that relies on the variations in the luminescence properties of a Zn(II) based MOF, namely MAF-34 or $[Zn_7(ip)_{12}](OH)_2$ where ip = 1*H*-imidazo[4,5-*f*][1,10] phenanthroline, upon interaction with CO_2 molecules. The crystalline structure of this flexible MOF is strongly affected by the presence of guest molecules in the pores. When loaded with guest molecules, the strain applied on the crystal structure of the framework prevents linker–linker interactions, effectively shifting the λ_{max} of its fluorescent emission. Thus, low-pressure CO_2 adsorption shifts the emission color from strong cyan photoluminescence (λ_{max} = 487 nm) to yellowish orange (λ_{max} = 540 nm).[70] The sensing response was observed for three repeated cycles. MAF-34 also displayed sensing capability for vapours of various solvents (*e.g.*, benzene, nitrobenzene, ethanol) and further testing showed that thin films of the MOF can be grown on substrates while retaining their fluorescence, a significant advantage for device-integration.[70]

Tank *et al.*[71] used post-synthetic modification techniques to tune the chemical composition of UiO-66, also known as $Zr_6O_4(OH)_4(bdc)_6$ where bdc = 1,4-benzenedicarboxylate, by effectively integrating sodium phenolic functional groups within the pores of the MOF. The modified UiO-66, known as UiO-66-ONa, displays excellent sensitivity for CO_2 as the sodium phenolic moieties are transformed into OH groups upon reacting with CO_2 molecules. The respective fluorescence bands of UiO-66-ONa and UiO-66-OH are shifted by 50 nm. Therefore, by measuring the fluorescence spectra of a suspension of the MOF powder, one can probe the CO_2 concentration in the surrounding atmosphere. Using this method, it was obtained a LoD of 3.5×10^{-7} M and a response time of *ca.* 65 seconds. The advantages of this material include strong chemical selectivity towards CO_2, a well-studied and relatively easy synthesis procedure and excellent stability. On the other hand, using a suspension is unpractical for device integration and the recycling protocol, involving exposure to NaOH to convert UiO-66-OH back to UiO-66-ONa, suggests that the MOF probe is pH sensitive which could limit its effectiveness. Nevertheless, further development could overcome the aforementioned limitations and the concept of a CO_2 sensor built on a well-known and robust MOF, which can be made using easy synthesis methods and with significant potential for chemical tuneability, is very promising. Furthermore, such method could virtually be used to probe any analyte provided that several requirements are fulfilled: the effective diameter of the analyte is small enough for it to access the pores, the functional group shows selective chemical reactivity with the analyte and the luminescence properties of the MOF before and after the reaction is significant enough to be measured accurately.

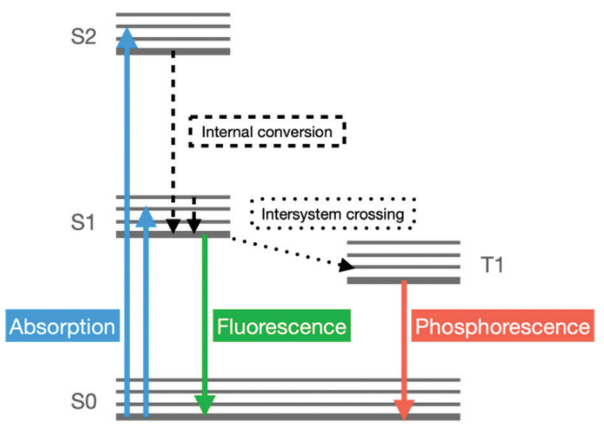

Fig. 9 Perrin–Jablonski diagram of luminescence processes.

Challenges associated with the integration of MOFs in devices

The integration of MOFs into devices remains one of the major hindrances to the development of mass fabricated and everyday use MOF-based sensors. The problem partly originates from the poor performances of many of these hybrid materials in open atmosphere due to water interference (detection of water molecules instead of analyte) or their low water stability as they tend to hydrolyse under humid conditions.[75,76]

Chocarro-Ruiz *et al.*[72] provide a good example of how to tackle the humidity problem by making the deliberate decision

to prioritise stability over sensitivity for increased durability. They used ZIF-8 nanoparticles, which are known to be water stable, as sensing component in a bimodal waveguide interferometric sensor that detects small fluctuations of the refractive index due to the interaction between an analyte and a sensing material. The sensor displays a linear response to CO_2 concentrations varying from 1 vol% to 100 vol%, CO_2 selectivity over water and CH_4 and good stability as the sensor remained efficient after being stored 1 month in air (or 1 day at 80% RH). The LoD of 3130 ppm at room temperature (down to 774 ppm at 278 K), although relatively high compared to other MOF-based sensors, is suitable for multiple real-life applications. Moreover, the sensor showed constant performances through 50 consecutive measurements and reproducible performances from batch to batch.

While Chocarro-Ruiz *et al.*[72] demonstrated the value of choosing a stable MOF as sensing component despite of higher LoD, tailoring the properties of MOFs to improve their stability remains a powerful approach for designing sensing materials with potential for real-life applications. This is supported by the studies of Kim *et al.*[73] (discussed below) and Pentyala *et al.*[24] (discussed above). Nevertheless, other hurdles regarding synthesis often remain for water-stable MOFs (*e.g.*, ZIF-8, UiO-66, lanthanide-based MOFs)[72,77] or MOFs species rendered water-stable through structural and/or chemical tuning (*e.g.*, DMOF-1, MOF-74),[73,78] especially when grown as thin films on substrates. These limitations stem from our poor understanding of the influence that both intrinsic properties of the MOF specimen and synthesis conditions have over the properties (*e.g.*, thickness, crystalline orientation, roughness, homogeneity) of the subsequent thin film. Thus, to be able to grow these so-called surface-mounted metal–organic frameworks (SURMOFs) with high level of control over their aforementioned properties, extensive optimisation procedures are required for every MOF specimen. In addition to nucleation and growth mechanisms, the interaction between a SURMOF and its substrate is another crucial – yet misunderstood – phenomenon for an effective synthesis, long-term stability and overall efficiency of the device that rely on that SURMOF to operate. Thus, the incorporation of MOFs as full-fledged electronic components in devices still lags as many prototypes rely on loose single crystals or powders while other applications remain currently unrealistic. These considerations advocate for more experimental and theoretical investigations to unravel the mechanisms of nucleation, growth and general synthesis of MOFs and SURMOFs.

One of the few studies tackling the complexity of MOFs' growth on solid surfaces was conducted by Kim *et al.*[73] and it is focused on a series of pillar-layer SURMOFs based on $Cu_2(bdc)_2(dabco)$ (bdc = 1,4-benzenedicarboxylic acid; dabco = 1,4-diazabicyclo[2.2.2]octane), also known as DMOF-1. Various analogues of DMOF-1 with different functionalised versions of its bdc linker were grown directly on hydroxy double salt (HDS) surfaces composed of copper-doped and aluminium-doped ZnO. It was shown that aside from the type of linker used, the growth conditions, *i.e.*, reaction time and linker ratio, also affect the properties of the films (*e.g.*, thickness, crystalline orientation, roughness). Although, as other studies showed, the exact influence of the synthesis parameters on their properties is not well understood, the authors successfully developed a synthetic procedure that yields homogeneous thin films of $Cu_2(bdc)_2(dabco)$ and its analogues at ambient conditions and on cm-scale substrates. It was also examined the potential of $Cu_2(nbdc)_2(dabco)$, where nbdc = 1,4-napthalenedicarboxyic acid, as a CO_2 sensing material for quartz crystal microbalance (QCM) and optical fibre techniques. This MOF displayed promising CO_2 sensing properties using both techniques, being able to detect up to 10 vol% of CO_2, even at 56% RH, with strong CO_2 selectivity (as compared to O_2, H_2, CH_4 and N_2 gases).

The CO_2 (and SF_6) sensor based on localized surface plasmon resonance (LSPR) spectroscopy and developed by Kreno *et al.*[74] follows relatively easy fabrication protocols. It consists of an extended pattern of Ag nanoarray coated with a thin film of HKUST-1 as sensing component. The arrays of Ag nanoparticles are fabricated using nanosphere lithography[79] whilst the film of HKUST-1 is obtained using a LbL liquid phase epitaxy (LPE) method,[80] both well-known and relatively easy techniques with potential for high-throughput fabrication. Due to the enhancement factor provided by the presence of LSPs, the system can detect small variations in the refractive index of the thin film of HKUST-1 upon its interaction with CO_2 molecules. The sensor showed successful CO_2 detection within a few seconds for a concentration of 10 vol% CO_2. Nevertheless, it is important to note that the reported data suggest that much lower LoD could be reached. While similar concepts with better sensing capabilities were discussed, the simplicity of the fabrication method and the room for improvement, in particular the sensing performances of the MOF, make this sensor attractive for inexpensive and large-scale manufacturing.

Lastly, as the aforementioned work from Chocarro-Ruiz *et al.*[72] already suggested, researchers should keep their designs and fabrication methods simple as much as possible to enable reproduceable and scalable manufacturing. Yet, the importance of this argument should be nuanced in the case of devices showing exceptional sensing performances or unique capabilities or functionalities. Moreover, as the field of MOF-based sensing continuous to grow, overlooked properties such as the size of the sensor device, its power consumption, and electronics overheads will require increasing attention.[81]

Conclusions

Rigorous safety regulations for both indoor air quality and environmental exhaust from industrial processes have led to increased research focused on the development of effective gas sensors. All current technologies for CO_2 sensing have their own set of advantages and limitations that make them relevant for specific sensing applications. For instance, devices based on optical detection have high sensitivity although they suffer from water interferences, polymer-based chemical sensors are produced relatively cheaply yet have shorter operating life and conductometric metal-oxide sensors are limited by their high

operating temperatures despite that they enable the fabrication of portable instruments.

MOFs are promising sensing layers for selective and sensitive CO_2 detection as a result of their extremely high surface area, relatively wide range of operating temperatures (relevant for practical applications) as well as their structural and chemical tunability. Especially, the possibility to tailor the properties of MOFs enables synthetic chemists to gain control over the MOF–CO_2 interactions by fine-tuning the pore sizes and/or active sites of these materials through meticulous selection of organic and inorganic parts and advanced MOF functionalization. From this perspective, we have discussed the different transducers used by researchers to design prototypes or develop proofs of concept for MOF-based sensors for CO_2 detection. The challenges associated with the integration of MOFs as central components in sensing devices are also discussed. These challenges, mostly linked to the low hydrolytic stability and the general lack of understanding of the growth mechanisms of MOFs as thin layers, hold back the transition of MOF-based CO_2 sensing devices from laboratory prototypes to off-the-shelf items.

We strongly believe that the potential of MOFs for chemical sensing applications justifies the research efforts to solve the aforementioned hurdles (and others like toxicity, low electrical conductivity, poor mechanical stability, *etc.*) or to optimize the existing prototypes. Thus, we advocate for further studies on these materials in relation not only to CO_2 sensing, but also in relation to other relevant chemical sensing applications (such as H_2S, NH_3, N_2O, volatile organic compounds and explosive sensing), as any insight would be beneficial for the development of MOF-based technologies.

Author contributions

Dr Andreea Gheorghe and Olivier Lugier contributed equally to this work in terms of logic, content construction and writing. Bohui Ye contributed to the literature search and writing parts of the article. Dr Stefania Tanase guided the writing of the article in terms of the topic, content structure and core components and contributed to the writing.

Conflicts of interest

There are no conflicts to declare.

Acknowledgements

This work is also part of the Research Priority Area Sustainable Chemistry of the University of Amsterdam, http://suschem.uva.nl.

Notes and references

1 J. Bongaarts, *Popul. Dev. Rev.*, 1992, **18**, 299–319.
2 J. C. Pales and C. D. Keeling, *J. Geophys. Res.*, 1965, **70**, 6053–6076.
3 M. McGee, CO2 Records, https://www.co2.earth/co2-records, (accessed May 7, 2021).
4 K. Huttunen, in *Clinical Handbook of Air Pollution-Related Diseases*, ed. F. Capello and A. V. Gaddi, Springer International Publishing, Cham, 2018, pp. 107–114.
5 Industrial Scientific, The Gas Detection People, Carbon Dioxide Gas Detectors, http://www.indsci.com/products/carbon-dioxide/, (accessed April 2, 2018).
6 W. J. Fisk, D. Faulkner and D. P. Sullivan, *Accuracy of CO2 sensors in commercial buildings: a pilotstudy*, Ernest Orlando Lawrence Berkeley NationalLaboratory, Berkeley, CA (US), 2006.
7 Edaphic, http://www.edaphic.com.au/knowledge-base/articles/gas-articles/ndir-explained/, (accessed July 3, 2018).
8 Y.-W. Sun, Y. Zeng, W.-Q. Liu, P.-H. Xie, K.-L. Chan, X.-X. Li, S.-M. Wang and S.-H. Huang, *Chin. Phys. B*, 2012, **21**, 090701.
9 C. Mitra, *Infrared Spectroscopy – Principles, Advances, and Applications*, IntechOpen, 2018, pp. 5–12.
10 T.-V. Dinh, I.-Y. Choi, Y.-S. Son and J.-C. Kim, *Sens. Actuators, B*, 2016, **231**, 529–538.
11 C. Chen, J. Kim and W.-S. Ahn, *Korean J. Chem. Eng.*, 2014, **31**, 1919–1934.
12 S. Lin and P. Theato, *Macromol. Rapid Commun.*, 2013, **34**, 1118–1133.
13 S. Srinives, T. Sarkar, R. Hernandez and A. Mulchandani, *Anal. Chim. Acta*, 2015, **874**, 54–58.
14 X. Liu, S. Cheng, H. Liu, S. Hu, D. Zhang and H. Ning, *Sensors*, 2012, **12**, 9635–9665.
15 G. F. Fine, L. M. Cavanagh, A. Afonja and R. Binions, *Sensors*, 2010, **10**, 5469–5502.
16 S. M. Kanan, O. M. El-Kadri, I. A. Abu-Yousef and M. C. Kanan, *Sensors*, 2009, **9**, 8158–8196.
17 J. Zhang, Z. Qin, D. Zeng and C. Xie, *Phys. Chem. Chem. Phys.*, 2017, **19**, 6313–6329.
18 A. Tricoli, M. Righettoni and A. Teleki, *Angew. Chem., Int. Ed.*, 2010, **49**, 7632–7659.
19 G. Korotcenkov, *Handbook of Gas Sensor Materials*, Springer, New York, NY, 2013.
20 Z. Ahmad, S. Manzoor, M. Talib, S. S. Islam and P. Mishra, *Mater. Sci. Eng., B*, 2020, **255**, 114528.
21 E. Singh, M. Meyyappan and H. S. Nalwa, *ACS Appl. Mater. Interfaces*, 2017, **9**, 34544–34586.
22 M. Schleicher and M. Fyta, *ACS Appl. Electron. Mater.*, 2020, **2**, 74–83.
23 I. G. Giannakopoulos, D. Kouzoudis, C. A. Grimes and V. Nikolakis, *Adv. Funct. Mater.*, 2005, **15**, 1165–1170.
24 V. Pentyala, P. Davydovskaya, R. Pohle, G. Urban and O. Yurchenko, *Procedia Eng.*, 2014, **87**, 1071–1074.
25 P. Freund, L. Mielewczyk, M. Rauche, I. Senkovska, S. Ehrling, E. Brunner and S. Kaskel, *ACS Sustainable Chem. Eng.*, 2019, **7**, 4012–4018.
26 H. Yuan, J. Tao, N. Li, A. Karmakar, C. Tang, H. Cai, S. J. Pennycook, N. Singh and D. Zhao, *Angew. Chem., Int. Ed.*, 2019, **58**, 14089–14094.
27 N. Wang, A. Mundstock, Y. Liu, A. Huang and J. Caro, *Chem. Eng. Sci.*, 2015, **124**, 27–36.
28 H.-C. Zhou, J. R. Long and O. M. Yaghi, *Chem. Rev.*, 2012, **112**, 673–674.

29 N. C. Burtch, J. Heinen, T. D. Bennett, D. Dubbeldam and M. D. Allendorf, *Adv. Mater.*, 2018, **30**, 1704124.
30 S. Jung, L. Huelsenbeck, Q. Hu, S. Robinson and G. Giri, *ACS Appl. Mater. Interfaces*, 2021, **13**, 10202–10209.
31 Y. Lin, C. Kong, Q. Zhang and L. Chen, *Adv. Energy Mater.*, 2017, **7**, 1601296.
32 K. Sumida, D. L. Rogow, J. A. Mason, T. M. McDonald, E. D. Bloch, Z. R. Herm, T.-H. Bae and J. R. Long, *Chem. Rev.*, 2012, **112**, 724–781.
33 R. Krishna and J. M. van Baten, *Sep. Purif. Technol.*, 2012, **87**, 120–126.
34 M. Dinca and J. R. Long, *J. Am. Chem. Soc.*, 2005, **127**, 9376–9377.
35 W. Zhuang, D. Yuan, D. Liu, C. Zhong, J.-R. Li and H.-C. Zhou, *Chem. Mater.*, 2012, **24**, 18–25.
36 K. K. Gangu, S. Maddila, S. B. Mukkamala and S. B. Jonnalagadda, *Inorg. Chim. Acta*, 2016, **446**, 61–74.
37 M. D. Allendorf, A. Schwartzberg, V. Stavila and A. A. Talin, *Chem. – Eur. J.*, 2011, **17**, 11372–11388.
38 L. E. Kreno, K. Leong, O. K. Farha, M. Allendorf, R. P. Van Duyne and J. T. Hupp, *Chem. Rev.*, 2012, **112**, 1105–1125.
39 H.-T. Kim, W. Hwang, Y. Liu and M. Yu, *Opt. Express*, 2020, **28**, 29937.
40 R. Islam, M. M. Ali, M.-H. Lai, K.-S. Lim and H. Ahmad, *Sensors*, 2014, **14**(4), 7451–7488.
41 K. A. Willets and R. P. Van Duyne, *Annu. Rev. Phys. Chem.*, 2007, **58**, 267–297.
42 J. Homola, S. S. Yee and G. Gauglitz, *Sens. Actuators, B*, 1999, **54**, 3–15.
43 X. Chong, Y. Zhang, E. Li, K.-J. Kim, P. R. Ohodnicki, C. Chang and A. X. Wang, *ACS Sens.*, 2018, **3**, 230–238.
44 K. Huang, S. Gong, L. Zhang, H. Zhang, S. Li, G. Ye and F. Huang, *Chem. Commun.*, 2021, **57**, 2144–2147.
45 Chemistry Libre Texts Library, Infrared spectroscopy, https://chem.libretexts.org/Core/Physical_and_Theoretical_Chemistry/Spectroscopy/Vibrational_Spectroscopy/Infrared_Spectroscopy, (accessed April 4, 2018).
46 International sensor technology, Infrared gas sensor, http://www.intlsensor.com/pdf/infrared.pdf, (accessed April 5, 2018).
47 B. Lee, *Opt. Fiber Technol.*, 2003, **9**, 57–79.
48 X. Chong, K.-J. Kim, P. R. Ohodnicki, E. Li, C.-H. Chang and A. X. Wang, *IEEE Sens. J.*, 2015, **15**, 5327–5332.
49 X. Chong, K.-J. Kim, E. Li, Y. Zhang, P. R. Ohodnicki, C.-H. Chang and A. X. Wang, *Sens. Actuators, B*, 2016, **232**, 43–51.
50 X. Wang and O. S. Wolfbeis, *Anal. Chem.*, 2020, **92**, 397–430.
51 K. Wysokiński, M. Napierała, T. Stańczyk, S. Lipiński and T. Nasiłowski, *Sensors*, 2015, **15**, 31888–31903.
52 J. Hodgkinson and R. P. Tatam, *Meas. Sci. Technol.*, 2012, **24**, 012004.
53 Novocontrol, Dielectric Spectroscopy, Conductivity Spectroscopy, and Electrochemical Impedance Spectroscopy, http://www.novocontrol.de/php/intro_overview.php, (accessed April 19, 2018).
54 I. Strauss, A. Mundstock, M. Treger, K. Lange, S. Hwang, C. Chmelik, P. Rusch, N. C. Bigall, T. Pichler, H. Shiozawa and J. Caro, *ACS Appl. Mater. Interfaces*, 2019, **11**, 14175–14181.
55 I. Stassen, J.-H. Dou, C. Hendon and M. Dincă, *ACS Cent. Sci.*, 2019, **5**, 1425–1431.
56 C. Liu, Y. Gu, C. Liu, S. Liu, X. Li, J. Ma and M. Ding, *ACS Sens.*, 2021, **6**, 429–438.
57 M. E. DMello, N. G. Sundaram and S. B. Kalidindi, *Chem. – Eur. J.*, 2018, **24**, 9220–9223.
58 L. Liu, Y. Zhou, S. Liu and M. Xu, *ChemElectroChem*, 2018, **5**, 6–19.
59 N. C. Jeong, B. Samanta, C. Y. Lee, O. K. Farha and J. T. Hupp, *J. Am. Chem. Soc.*, 2012, **134**, 51–54.
60 A. Shigematsu, T. Yamada and H. Kitagawa, *J. Am. Chem. Soc.*, 2011, **133**, 2034–2036.
61 B. Ye, A. Gheorghe, R. van Hal, M. Zevenbergen and S. Tanase, *Mol. Syst. Des. Eng.*, 2020, **5**, 1071–1076.
62 J. J. Gassensmith, J. Y. Kim, J. M. Holcroft, O. K. Farha, J. F. Stoddart, J. T. Hupp and N. C. Jeong, *J. Am. Chem. Soc.*, 2014, **136**, 8277–8282.
63 S. Tanase, M. C. Mittelmeijer-Hazeleger, G. Rothenberg, C. Mathonière, V. Jubera, J. M. M. Smits and R. de Gelder, *J. Mater. Chem.*, 2011, **21**, 15544–15551.
64 S. R. Caskey, A. G. Wong-Foy and A. J. Matzger, *J. Am. Chem. Soc.*, 2008, **130**, 10870–10871.
65 A. Lv, Y. Pan and L. Chi, *Sensors*, 2017, **17**, 213.
66 Kelvin Probe, http://www.kelvinprobe.info/technique-theory.htm, (accessed April 12, 2018).
67 N. A. Surplice and R. J. D'Arcy, *J. Phys. E: Sci. Instrum.*, 1970, **3**, 477–482.
68 V. Pentyala, P. Davydovskaya, M. Ade, R. Pohle and G. Urban, *Sens. Actuators, B*, 2016, **225**, 363–368.
69 M. D. Allendorf, C. A. Bauer, R. K. Bhakta and R. J. T. Houk, *Chem. Soc. Rev.*, 2009, **38**, 1330–1352.
70 X.-L. Qi, R.-B. Lin, Q. Chen, J.-B. Lin, J.-P. Zhang and X.-M. Chen, *Chem. Sci.*, 2011, **2**, 2214–2218.
71 Y. Tang, J. Chen, H. Wu, J. Yu, J. Jia, W. Xu, Y. Fu, Q. He, H. Cao and J. Cheng, *Dyes Pigm.*, 2020, **172**, 107798.
72 B. Chocarro-Ruiz, J. Pérez-Carvajal, C. Avci, O. Calvo-Lozano, M. I. Alonso, D. Maspoch and L. M. Lechuga, *J. Mater. Chem. A*, 2018, **6**, 13171–13177.
73 K.-J. Kim, J. E. Ellis, B. H. Howard and P. R. Ohodnicki, *ACS Appl. Mater. Interfaces*, 2021, **13**, 2062–2071.
74 L. E. Kreno, J. T. Hupp and R. P. Van Duyne, *Anal. Chem.*, 2010, **82**, 8042–8046.
75 N. Al-Janabi, P. Hill, L. Torrente-Murciano, A. Garforth, P. Gorgojo, F. Siperstein and X. Fan, *Chem. Eng. J.*, 2015, **281**, 669–677.
76 H. Jasuja, N. C. Burtch, Y. Huang, Y. Cai and K. S. Walton, *Langmuir*, 2013, **29**, 633–642.
77 X. Liu, N. K. Demir, Z. Wu and K. Li, *J. Am. Chem. Soc.*, 2015, **137**, 6999–7002.
78 S. Zuluaga, E. M. A. Fuentes-Fernandez, K. Tan, F. Xu, J. Li, Y. J. Chabal and T. Thonhauser, *J. Mater. Chem. A*, 2016, **4**, 5176–5183.
79 C. L. Haynes and R. P. Van Duyne, *J. Phys. Chem. B*, 2001, **105**, 5599–5611.
80 O. Shekhah, H. Wang, S. Kowarik, F. Schreiber, M. Paulus, M. Tolan, C. Sternemann, F. Evers, D. Zacher, R. A. Fischer and C. Wöll, *J. Am. Chem. Soc.*, 2007, **129**, 15118–15119.
81 D. M. Wilson, S. Hoyt, J. Janata, K. Booksh and L. Obando, *IEEE Sens. J.*, 2001, **1**, 256–274.

